Brazilian Journal
of Chemical
Engineering

ISSN 0104-6632
Printed in Brazil
www.abeq.org.br/bjche

Vol. 31, No. 01, pp. 211 - 227, January - March, 2014

BIOSORPTION STUDY OF Ni^{2+} AND Cr^{3+} BY *Sargassum filipendula*: KINETICS AND EQUILIBRIUM

A. A. Seolatto[1], T. D. Martins[2,4], R. Bergamasco[3], C. R. G. Tavares[3], E. S. Cossich[3] and E. A. da Silva[4*]

[1]School of Chemistry, Federal University of Goiás - UFG, P.O. Box, CEP: 74001-970, Goiânia - GO, Brazil.
[2]School of Chemical Engineering, University of Campinas,
Av. Albert Einstein 500, CEP: 13083-852, Campinas - SP, Brazil.
[3]Department of Chemical Engineering, State University of Maringá - UEM,
Av. Colombo 5790, CEP: 87020-900- Maringá - PR, Brazil.
[4]School of Chemical Engineering, Western State University of Paraná - UNIOESTE,
Phone: + (55) (45) 33797039; Fax: + (55) (45) 33797002, Rua da Faculdade 645,
Jardim La Salle, CEP: 85903-000, Toledo - PR, Brazil.
E-mail: edsondeq@hotmail.com

(Submitted: June 24, 2010 ; Revised: April 11, 2012 ; Accepted: May 2, 2013)

Abstract - In this work, the biosorption of Cr^{3+} and Ni^{2+} by *Sargassum filipendula* pre-treated with $CaCl_2$ was studied. Kinetic and equilibrium experiments were carried out for mono- and multi-component solutions in a batch reactor at pH 3.0 and 30 ºC. The results from the kinetic experiments showed that Cr^{3+} adsorbs slower than Ni^{2+}. This behavior was explained by means of a mechanistic analysis, which showed that Cr^{3+} uptake presented three adsorption stages, whereas Ni^{2+} adsorption presents only two. The mono-component equilibrium data, along with binary kinetic data obtained from mono-component experiments, showed that, although the kinetics for Cr^{3+} removal are slower, the biomass had a stronger affinity for this ion. Almost all Ni^{2+} is desorbed from the biomass as Cr^{3+} adsorbs. The binary equilibrium data also presented this behavior. The binary data was also modeled by using modified forms of the Langmuir, Jain and Snoeyink, and Langmuir-Freundlich isotherms. However, the prediction obtained presented low accuracy. An alternative modeling with artificial neural networks was presented and the results showed that this technique could be a promising tool to represent binary equilibrium data. The main contribution of this work was to obtain experimental data for Cr^{3+}/Ni^{2+} adsorption, which is a system rarely found in the literature and that provides information that could be used in process modeling and simulation.
Keywords: Algal biomass; Mathematical modeling; Neural networks; Single solution; Binary solution.

INTRODUCTION

Many industrial segments are responsible for the increasing amount of metallic ions released into the environment. For example, Cr^{3+} is released in wastewaters by several industrial sectors, such as mining, iron sheet cleaning, chrome plating, leather tanning, finishing industries, and wood preservation. It is known to be toxic if absorbed in excess by the human body and may cause serious health concerns. Ni^{2+} can be found mainly in wastewater from electroplating, electronics, and metal cleaning industries. Human contact with Ni^{2+} causes severe damage to lungs and kidneys, gastrointestinal distress, pulmonary fibrosis, renal edema, and skin dermatitis.

There are several unit operations that could be used to remove heavy metals from wastewaters, such as: flocculation, precipitation, electrolysis, crystal-

*To whom correspondence should be addressed

lization, adsorption, chemical precipitation etc. However, these methods often demand high initial and maintenance costs, have low inefficiency (especially at low concentrations), offer no regeneration, need large amount of chemicals, generate new types of contaminants etc. To overcome these problems and enhance the removal efficiency, research groups all over the world have focused their attention on biosorption processes. Indeed, these studies showed that biosorption could be a promising alternative for heavy metal removal (Farooq *et al*., 2010).

Biosorption is a method to remove target substances from solution by using living or non-living biomass, based on the interaction present between the two (Volesky and Holan, 1995). Due to its low cost in comparison with other technologies, high efficiency, and minimization of chemical or biological sludge, biosorption has received significant attention over the last years.

Experimental studies on biosorbent selection for heavy metal removal include bacteria, yeast, fungi, and algal and plant derived materials (Farooq *et al*., 2010; Vieira *et al*., 2012). Moreover, studies in which seaweed is used, especially the *Sargassum* species, confirm that this biomass can remove several metallic ions (chromium, cadmium, copper, nickel, zinc etc.) very efficiently (Rocha *et al*., 2006; Tsui *et al*., 2006; Al-Homaidan, 2008; Hajar, 2009; Sivaprakash *et al*., 2010).

The aim of this work was to perform kinetic and equilibrium studies of Cr^{3+} and Ni^{2+} biosorption from single and binary solutions, using *Sargassum filipendula* algal biomass as biosorbent.

MATERIALS AND METHODS

Biomass and Solutions Preparation

The biomass used in this work was the brown seaweed *Sargassum filipendula*, commonly found in the Brazilian coast. First, it was washed with deionized water and dried at 60 °C for 24 h. The biomass was then treated according to the methodology described by Matheickal *et al*. (1999) and Matheickal and Yu (1999). The dried biomass was then chopped and sieved to different fraction sizes. Dry particles with an average diameter of 2.20 mm were used in all sorption experiments.

Chromium and nickel solutions were prepared by dissolving chromium chloride hexahydrate ($CrCl_3.6H_2O$) and nickel chloride hexahydrate ($NiCl_2.6H_2O$) in deionized water.

Kinetic Studies

Kinetic experiments were carried out in 2 L Erlenmeyer flasks, containing 1 L of metal solution (Cr^{3+}, Ni^{2+} or their mixture) and 1.5 g of dry biomass. Among all parameters that affect the process kinetics, only heavy metal initial concentration is considered here. All the other parameters were kept fixed. The tests for the mono-component system were carried out with the following initial concentrations: 2 meq Ni^{2+}/L, 5 meq Ni^{2+}/L, 3 meq Cr^{3+}/L, 8 meq Cr^{3+}/L. For binary systems, the following initial concentrations were used: 4 meq Ni^{2+}/L and 8 meq Cr^{3+}/L (experiment 1), 2 meq Ni^{2+}/L and 6 meq Cr^{3+}/L (experiment 2), and 5 meq Ni^{2+}/L and 3 meq Cr^{3+}/L (experiment 3). The flasks were kept at 30 ºC under 200 rpm agitation. The pH was kept fixed at 3.0. During the experiments pH tends to rise, thus it was adjusted with a 1 M HCl solution whenever needed.

Equilibrium Studies

Equilibrium experiments in mono-component and binary systems of Cr^{3+} and Ni^{2+} were carried out in a batch reactor. For all experiments, the initial solution concentration ranged from 1 to 18 meq/L. Erlenmeyer flasks containing 0.23 g of dry biomass and 50 mL of each metallic ion solution were kept under constant agitation at 200 rpm in a rotary shaker, at a fixed temperature of 30 °C and pH 3. A solution of 1 M HCl was used to adjust the pH whenever needed. To ensure that the systems reached equilibrium, all the experiments lasted 72 hours.

Data Analysis

In all kinetic and equilibrium tests, the adsorbed amount of the corresponding ion (Cr^{3+} or Ni^{2+}) in the biosorbent (q_t) was calculated by the following equation:

$$q_t = \frac{V\left(C_0 - C_t\right)}{M} \tag{1}$$

where V is the volume of solution, C_0 is the initial concentration of ion in solution, C_t is the concentration of ion in solution at a time t, and M is the biosorbent's dry mass.

The ions concentrations in solution (Ni^{2+} and/or Cr^{3+}) were determined by atomic absorption spectrometry (Varian SpectrAA-10 plus). Standard solutions were prepared at concentrations of 0.05, 0.1, 0.2,

0.4, and 0.5 meq/L (Merck-Tritisol). All equilibrium sorption experiments were carried out in duplicate and the data presented here correspond to the average value.

RESULTS AND DISCUSSION

Kinetic Studies

Mono-Component System

Kinetics experiments are an important aspect that needs to be addressed in all sorption studies. A proper analysis of adsorption kinetics can provide information about the process speed, the time required to reach equilibrium, as well as some insights into the adsorption mechanisms. The results obtained in kinetic experiments for Ni^{2+} and Cr^{3+} biosorption are shown in Figure 1(a) and 1(b). Concentrations in the fluid phase are shown on the main axis and the amount of heavy metal adsorbed in the inset.

The kinetic data presented in these graphs haves a familiar behavior. The removal rate was high at the beginning followed by a rate decrease when the process approaches equilibrium. The kinetic rate became zero at the equilibrium. Besides, it seems that the initial heavy metal concentration had no significant effect on the kinetic rate. Cr^{3+} biosorption was slower than Ni^{2+} (in just one hour, around 85 % of Ni^{2+} and 62 % of Cr^{3+} was removed from the solution), and the total time required for its removal to reach equilibrium was about 7.5 times (~30 h) that required for Ni^{2+} (~4 h).

Cr^{3+} an Ni^{2+} kinetics can be explained using speciation diagrams. Fahim *et al*. (2006) presented a speciation diagram of chromium in the pH range of 2-12. According to this graph, an aqueous solution of pH 3.0 has approximately 80% and 20% of Cr^{3+} and $CrOH^{2+}$ ions, respectively. Srivastava *et al*. (2009) stated that, in a similar solution, Ni^{2+} ions are predominant. It is possible that the lower adsorption rate of chromium ions is due the presence of $CrOH^{2+}$, which presents lower diffusivity than Cr^{3+} and Ni^{2+}.

To quantify the kinetic aspects of biosorption, mathematical modeling has been used in several studies over the years. To obtain as much information as possible about the Ni^{2+} and Cr^{3+} biosorption kinetics, we modeled the experimental data obtained by using four theoretical models: pseudo-first-order (Lagergren, 1898), pseudo-second-order (Ho and McKay, 1998), three-stage (Choi *et al*., 2007), and the intra-particle diffusion model (Ruthven, 1984).

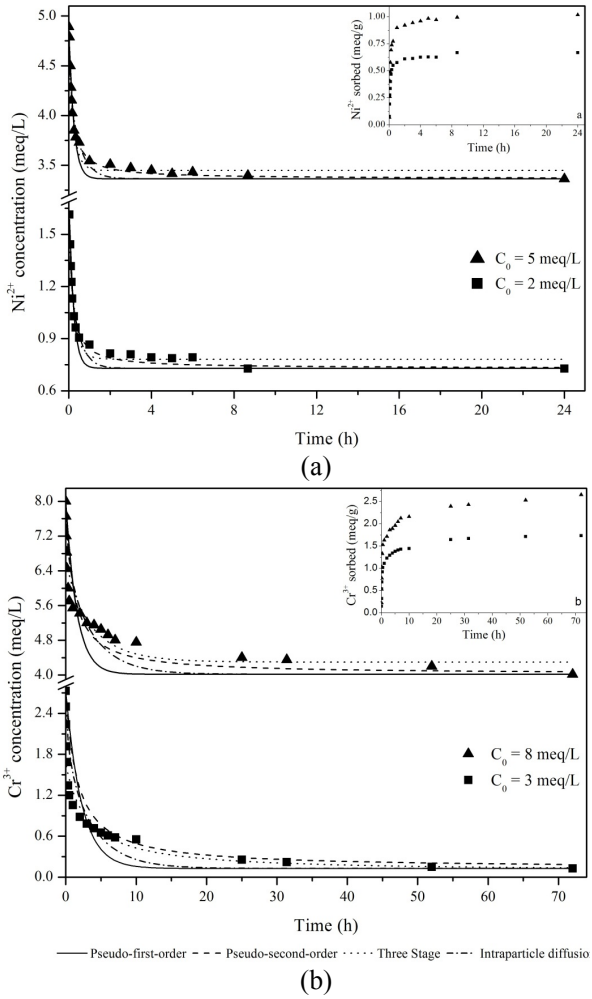

Figure 1: Kinetic curves for (a) Ni^{2+} and (b) Cr^{3} obtained in mono-component experiments.

The pseudo-first-order model is expressed by the differential equation:

$$\frac{dq_t}{dt} = k_1(q_{eq} - q_t) \tag{2}$$

where: q_t and q_{eq} are the amount adsorbed at the time t and at equilibrium, respectively (meq.g^{-1}), k_1 is the pseudo-first-order kinetic rate parameter (s^{-1}), and t is the time (s). Integrating Eq. (2) between *0* and t, and *0* and q, it becomes:

$$q_t = q_{eq}\left(1 - e^{-k_1 t}\right) \tag{3}$$

The pseudo-second-order model is expressed as:

$$\frac{dq_t}{dt} = k_2\left(q_{eq} - q_t\right)^2 \tag{4}$$

where: k_2 is the pseudo-second-order kinetic rate parameter (g. meq^{-1}.s^{-1}). Similarly, an explicit equation for q_t can be obtained by integrating Eq. (4) between *0* and *t*, and *0* and *q*:

$$q_t = \frac{k_2 q_{eq}^2 t}{1 + k_2 q_{eq} t} \tag{5}$$

In order to explain different adsorption mechanisms, Wilczak and Keinath (1993) proposed a new model based on three-stage kinetics. Figure 2 illustrates how this process occurs.

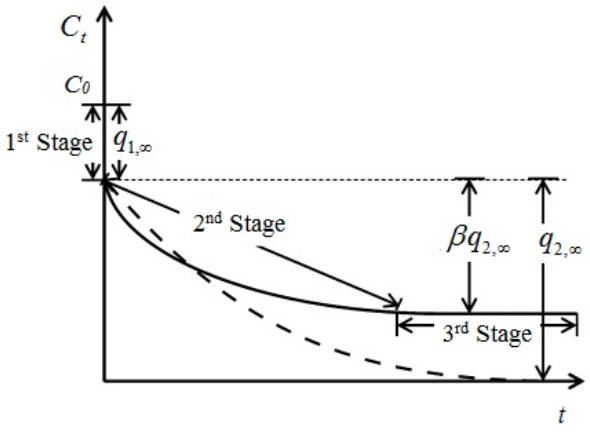

Figure 2: Illustration of a three-stage adsorption process. Adapted from Choi *et al*. (2007).

According to the authors, the first step is an instantaneous and irreversible adsorption on the adsorbent exterior surface (type-1 sites). Mathematically, it can be described by the equation:

$$q_t = q_{1,\infty} \tag{6}$$

where $q_{1,\infty}$ is the maximum amount that can be adsorbed on type-1 sites. The second step is a slow intra-particle adsorption at type-2 sites described by the equation:

$$\frac{\partial C_t}{\partial t} = -\alpha C_t \left[1 - \frac{q_t}{\beta q_{2,\infty}} \right] \tag{7}$$

where α is the rate constant for mass transfer from the fluid phase to the interior sites (s^{-1}), $q_{2,\infty}$ is the maximum amount adsorbed at type-2 sites (meq.g^{-1}), and β is a limiting factor for $q_{2,\infty}$ that lies in the [0;1] range (dimensionless). $\beta = 0$ is characteristic of an instantaneous adsorption only, whereas $\beta = 1$ defines two-stage adsorption kinetics. A three-stage kinetic process takes place when $\beta \in (0,1)$. In this case, the ion concentration in the fluid phase does not approach zero at the end of the experiment. Instead, the type-2 adsorption is suppressed by some mass transfer barrier (such as: small particle size, high fluid phase concentration) at a time *t* and the amount of adsorbed material at type-2 sites is a fraction β different from the values of one theoretically possible.

Integrating Eq. (7), along with the mass balance for the system, the analytical solution can be obtained (details can be found in Wilczak and Keinath (1993)):

$$C_t = \frac{C_0(1-\xi_1)(1-\xi_1-\beta\xi_2)}{1-\xi_1-\beta\xi_2 e^{-\gamma t}} \tag{8}$$

where:

$\xi_1 = \frac{M q_{1,\infty}}{V C_0}$ is the fraction of the ion adsorbed at type-1 sites, $\xi_2 = \frac{M q_{2,\infty}}{V C_0}$, is the fraction of the ion adsorbed at type-2 sites, and $\gamma = (1-\xi_1-\beta\xi_2)\alpha/\beta\xi_2$.

The constant effective diffusion model was previously described by Ruthven (1984). It is based on the mass balance for the solid phase and the following hypotheses are considered: the particle has a spherical form, the equilibrium concentration in the fluid phase does not differ much from its initial concentration, and heat transfer between the particle and the surrounding fluid is rapid, so temperature gradients can be considered to be negligible. Mathematically, this model can be expressed by the differential equation:

$$\frac{\partial q}{\partial t} = \frac{1}{r^2}\frac{\partial}{\partial}\left(r^2 D_{eff} \frac{\partial q}{\partial r} \right) \tag{9}$$

with the following initial and boundary conditions:

$$q(r,0) = 0 \tag{10}$$

$$q(r_p,t) = q_0 \tag{11}$$

$$\left.\frac{\partial q}{\partial r}\right|_{r=0} = 0 \tag{12}$$

An analytical solution for Eqs. (9)-(12) can be

derived and is given by (Ruthven, 1984):

$$\frac{\overline{q}}{q_0} = 1 - \frac{6}{\pi^2}\sum_{n=1}^{\infty}\frac{1}{n^2}\exp\left(-\frac{n^2\pi^2 D_{eff}\,t}{r_p^2}\right) \quad (13)$$

In Equations (9)-(13), r_p is the particle radius (cm), D_{eff} is the constant effective diffusion coefficient ($cm^2.s^{-1}$), n is the number of terms of the infinite series, q_0 is the amount adsorbed at the particle surface, in equilibrium with the fluid phase, and $\overline{q}$ is the average concentration through the particle ($meq.g^{-1}$):

$$\overline{q} = \frac{3}{r_p^3}\int_0^{r_p} q_t r^2 dr \quad (14)$$

The kinetic parameters of all models considered here were determined by using the Nelder and Mead (1965) method to minimize the objective function:

$$F_{OBJ} = \sum_{j=1}^{N}\left(\frac{C_{t,j}^{EXP} - C_{t,j}^{MOD}}{C_{t,j}^{EXP}}\right)^2 \quad (15)$$

where N is the total number of samples collected in the experiments. The superscripts *EXP* and *MOD* correspond to experimental and calculated data, respectively. After the adjustments, the accuracy of the kinetic models was evaluated by comparing some statistical parameters such as: average absolute deviation – defined by Eq. (16) – and correlation coefficients. To estimate D_{eff} in the intra-particle diffusion model, 5000 terms of the infinite series were considered.

$$AAD = \frac{1}{N}\left|\sum_{j=1}^{N}\frac{C_{t,j}^{Exp} - C_{t,j}^{Mod}}{C_{t,j}^{Exp}}\right| \quad (16)$$

All estimated kinetic parameters and the statistical parameters calculated for the kinetic modeling are shown in Table 1. The curves obtained from the models are also present in Figure 1. The parameter values showed that the initial concentration indeed influenced the removal kinetics. In general, kinetic parameters for Ni^{2+} decreased as C_0 increased. The opposite behavior occurred for Cr^{3+} removal. Our results are in agreement with several recent studies which present the same pattern of Ni^{2+} and Cr^{3+} removal, even when using different types of adsorbents (Nehrenheim and Gustafsson, 2008; Calero *et al*., 2009; Karaoğlu *et al*., 2010; Anoop Krishnan *et al*., 2011; Fernandes and Gando-Ferreira, 2011; Suazo-Madrid *et al*., 2011; Alomá *et al*., 2012).

Table 1: Adjusted and statistical parameters obtained for each kinetic model.

Model	Parameters			
	Ni^{2+}		Cr^{3+}	
Experimental conditions	$C_0 = 2$ $q_{eq} = 0.67$	$C_0 = 5$ $q_{eq} = 1.02$	$C_0 = 3$ $q_{eq} = 1.73$	$C_0 = 8$ $q_{eq} = 2.66$
First-order	$k_1 = 1.29\text{x}10^{-3}$ AAD = 5.37 $r^2 = 0.95$	$k_1 = 1.18\text{x}10^{-3}$ AAD = 2.15 $r^2 = 0.95$	$k_1 = 1.23\text{x}10^{-4}$ AAD = 40.43 $r^2 = 0.46$	$k_1 = 1.78\text{x}10^{-4}$ AAD = 11.89 $r^2 = 0.47$
Second-order	$k_2 = 3.27\text{x}10^{-3}$ AAD = 3.35 $r^2 = 0.98$	$k_2 = 1.86\text{x}10^{-3}$ AAD = 1.04 $r^2 = 0.98$	$k_2 = 9.81\text{x}10^{-5}$ AAD = 32.19 $r^2 = 0.57$	$k_2 = 1.49\text{x}10^{-4}$ AAD = 7.56 $r^2 = 0.79$
Three-stage	$\xi_1 = 1.00\text{x}10^{-4}$ $\xi_2 = 9.99\text{x}10^{-1}$ $\beta = 5.48\text{x}10^{-1}$ $\gamma = 8.47\text{x}10^{-4}$ AAD = 3.60 $r^2 = 0.95$	$\xi_1 = 6.4\text{x}10^{-4}$ $\xi_2 = 9.94\text{x}10^{-1}$ $\beta = 2.95\text{x}10^{-1}$ $\gamma = 1.06\text{x}10^{-3}$ AAD = 1.35 $r^2 = 0.97$	$\xi_1 = 3.88\text{x}10^{-1}$ $\xi_2 = 6.12\text{x}10^{-1}$ $\beta = 9.33\text{x}10^{-1}$ $\gamma = 6.65\text{x}10^{-5}$ AAD = 12.41 $r^2 = 0.84$	$\xi_1 = 1.70\text{x}10^{-1}$ $\xi_2 = 8.30\text{x}10^{-1}$ $\beta = 3.52\text{x}10^{-1}$ $\gamma = 5.92\text{x}10^{-5}$ AAD = 4.81 $r^2 = 0.87$
Intraparticle	$D_{eff} = 3.19\text{x}10^{-6}$ AAD = 5.50 $r^2 = 0.93$	$D_{eff} = 2.67\text{x}10^{-6}$ AAD = 2.05 $r^2 = 0.94$	$D_{eff} = 3.39\text{x}10^{-7}$ AAD = 25.94 $r^2 = 0.80$	$D_{eff} = 3.47\text{x}10^{-7}$ AAD = 5.50 $r^2 = 0.79$

$[C_0] = meq.L^{-1}$; $[q_{eq}] = meq.g^{-1}$; $[k_1] = s^{-1}$; $[k_2] = g.meq^{-1}.s^{-1}$; $[\xi_1] = [\xi_2] = [\beta]$ = dimensionless; $[\gamma] = s^{-1}$; $[D_{eff}] = cm.s^{-1}$; [AAD] = %

The statistical parameters obtained show that all models were in good agreement with the experimental data, the maximum calculated AADs were 5.50%. The pseudo-second-order and three stage models best fit the experimental data for Ni^{2+} and Cr^{3+} removal, respectively. These models presented the lowest AAD and the highest correlation coefficient among all models tested.

This result raises an important question: "What's the difference between Ni^{2+} and Cr^{3+} kinetic removal?" The answer to this question could be found by analyzing the mechanisms involved in the process. One way to perform this task is by using the pore-diffusion model proposed by Weber and Morris (1963). The authors suggested that sorption processes involve three main steps: (i) diffusion in the liquid film, (ii) pore diffusion and (iii) adsorption at the available sites. The one which occurs slowly is said to be the rate-limiting step and corresponds to the speed of the process. The last step (iii) is assumed to occur rapidly and therefore it is considered to be negligible.

To evaluate whether steps (i) or (ii) are the rate-controlling factor, one should plot and analyze q_t x $t^{0.5}$. If the plot behaves linearly, i.e.:

$$q_t = k_D \sqrt{t} + C \tag{17}$$

Then intra-particle diffusion is the rate-limiting step. In Eq. (17), k_D is the intra-particle diffusion coefficient (meq.g^{-1}.s$^{-0.5}$) and C (meq.g^{-1}) is a parameter that gives an idea about the boundary layer effect. A typical kinetic experiment usually leads to a plot with several linear segments, representing pore-diffusion in progressively smaller sizes. The equilibrium is represented by a horizontal line, where q_t is constant. The number of linear segments and which points belong to each segment can be chosen visually; however, this is not a reliable practice. Recently, Malash and El-Khaiary (2010) showed that the results obtained by applying Piecewise Linear Regression (PLR) are more accurate than the ones obtained by using the visual determination. In this work, the number of linear segments (and the boundaries between then) of the mono-component kinetic data were estimated by using the PLR technique. Details of the calculation procedures can be found in the original paper.

The linear segments obtained for the Ni^{2+} and Cr^{3+} kinetic data are shown in Figure 3. Table 2 shows the estimated parameters, the break times, and the correlation coefficients of each segment. The results show that the kinetic process was multi-linear for both metals. Besides, there is a clear difference between Cr^{3+} and Ni^{2+} removal: the number of adsorption stages. Three and two linear segments were calculated for Cr^{3+} and Ni^{2+}, respectively. This is confirmed by the high correlation coefficients obtained.

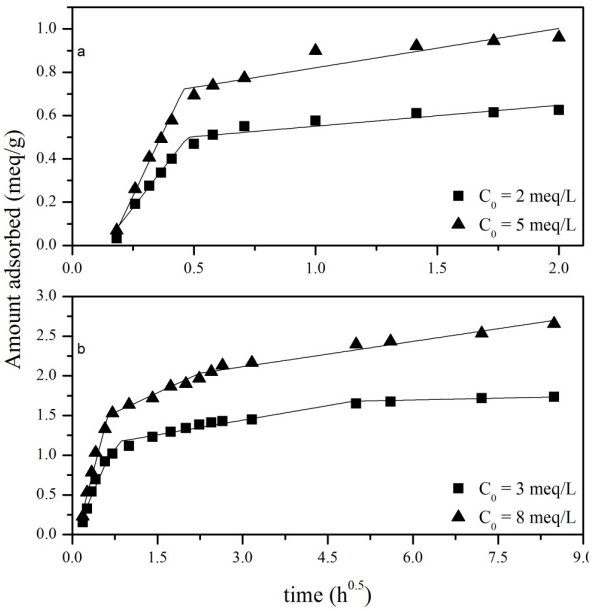

Figure 3: Pore-diffusion plots for (a) Ni^{2+} and (b) Cr^{3+} determined by PLR.

The first curve segment is often related to the external surface adsorption. It is generally the fastest part of the process, where the adsorbate diffuses through the bulk solution to the particle surface. When the surface reaches saturation, intra-particle diffusion takes place and the second curve segment forms. This stage is related to the macro-pore diffusion, where the intra-particle diffusion is the rate-controlling step on the adsorbent. A third curve segment is the equilibrium stage, where the adsorbate diffuses through the micro-pores. In this stage, the process slows down and the maximum adsorption is attained (Alkan *et al*., 2008). The description above is in perfect agreement with the k_D values presented in Table 2, where $k_{D,1} > k_{D,2} > k_{D,3}$. The results from the intra-particle model also confirmed that the initial concentration affect the process kinetics: for a different C_0, the diffusion parameters, as well as the break time values were also different.

Several authors reported the multi-step behavior of Cr^{3+} and Ni^{2+} adsorption using various different adsorbents (Oliveira *et al*., 2005; Nuhoglu and Malkoc, 2009; Chen *et al*., 2010; Ijagbemi *et al*., 2010; Karaoğlu *et al*., 2010; Aravindhan *et al*., 2012). In this work, Cr^{3+} biosorption occurs at the external surface and macro- and micro-pore regions, and Ni^{2+} biosorption occurs at the external surface and macro-pore region. This different multi-step behavior is the answer to the question addressed earlier.

Table 2: Results of PLR for the data shown in Figure 3.

System	Curve Segment								
	First			Second			Third		
Ni^{2+}	k_D	C	Break time	k_D	C	Break time	k_D	C	r^2
C_0 = 2	$2.28x10^{-2}$	$-1.70x10^{-1}$	0.28	$6.03x10^{-4}$	$5.33x10^{-1}$	-	-	-	0.982
C_0 = 5	$2.24x10^{-2}$	$5.53x10^{-2}$	0.52	$4.92x10^{-4}$	$8.94x10^{-1}$	-	-	-	0.981
Cr^{3+}									
C_0 = 3	$2.73x10^{-2}$	$-6.68x10^{-2}$	0.56	$2.04x10^{-3}$	1.07	24.5	$2.52x10^{-4}$	1.60	0.990
C_0 = 8	$4.71x10^{-2}$	$-2.19x10^{-1}$	0.36	$5.53x10^{-3}$	1.29	5.04	$1.78x10^{-3}$	1.79	0.995

[k_D] = $s^{-0.5}$; [C] = meq.g^{-1}; [Break time] = h;

Binary System

Industrial wastewaters often present more than one component. Thus, obtaining experimental data from multicomponent adsorption experiments is also important to evaluate the synergism that arises in such systems. In this work, kinetic experiments for Cr^{3+}/Ni^{2+} mixture biosorption were performed to evaluate the effect of Ni^{2+} over Cr^{3+} biosorption and vice-versa. The results obtained in these experiments are shown in Figure 4.

From this figure one can see that the time required for the system to reach equilibrium was 50 h. Besides, in the first two hours the biosorption rate for Ni^{2+} was higher than that for Cr^{3+}, which is comparable to the behavior observed in the mono-component kinetic runs. After this time, a significant amount of the adsorbed Ni^{2+} was replaced by Cr^{3+} ions and returned to the solution. The influence of Cr^{3+} ions on Ni^{2+} biosorption is clearly evident: the higher the Cr^{3+} initial concentration, the higher is the Ni^{2+} desorption from the biomass.

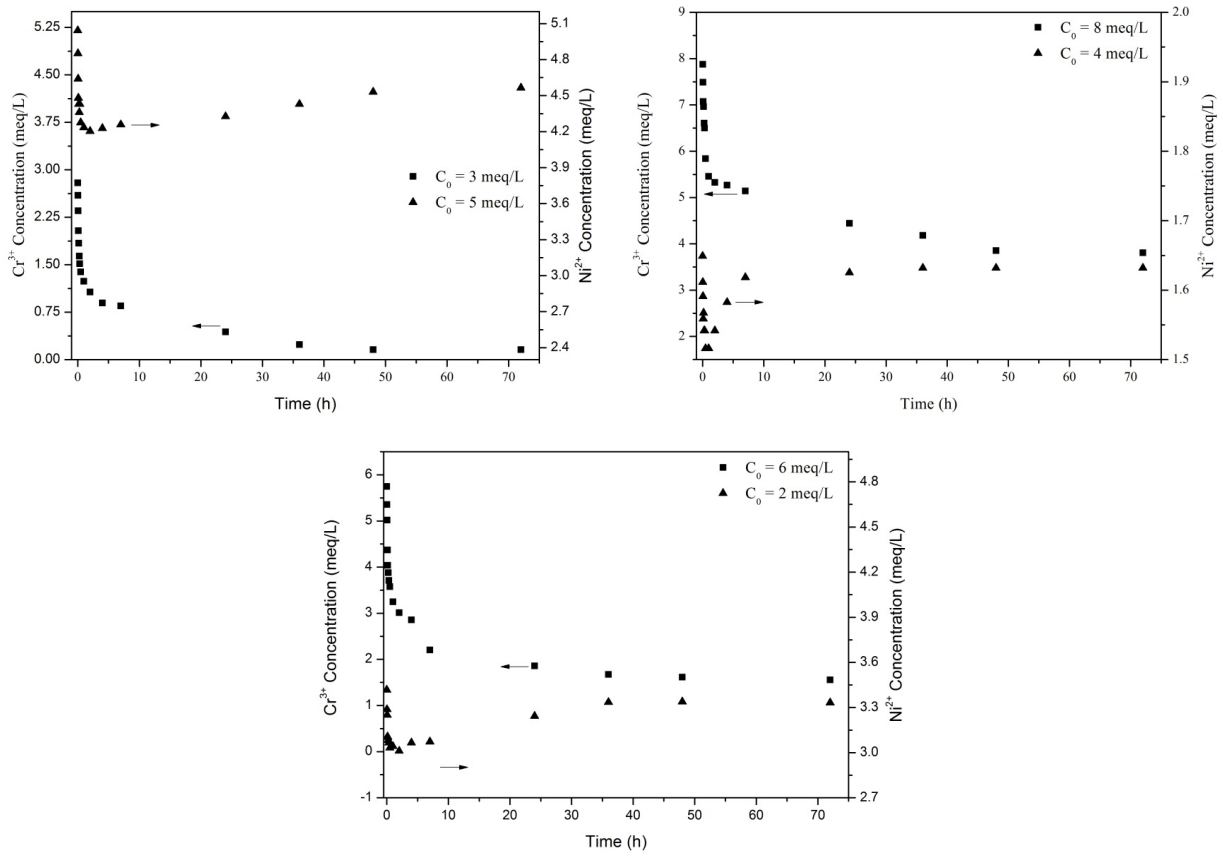

Figure 4: Kinetic curves for Ni^{2+} and Cr^{3+} biosorption obtained in the binary system experiments.

In these binary biosorption tests only 9.5%, 2.6%, and 1.2% of the Ni^{2+} ions were removed from the solution in experiments 1, 2, and 3 respectively. This probably occurred due to the competition for a determined adsorption site: Ni^{2+} has higher mobility and it adsorbs first, but since Cr^{3+} has a higher affinity to the adsorption sites, an ion exchange occurs and Ni^{2+} is desorbed.

Silva *et al*. (2003) studied the binary removal of Cr^{3+} and Cu^{2+} by *Sargassum sp.* in a batch reactor. The authors observed the same pattern presented here: that there was an initial biosorption of Cu^{2+}; however during the process, Cr^{3+} ions adsorbed onto the biosorbent surface, occupying the available sites and some of the sites previously occupied by Cu^{2+} ions. According to the authors, this replacement occurred due to the higher affinity of Cr^{3+} for the active sites.

Equilibrium Experiments

Mono-Component System

The first step in the design of adsorption/ biosorption processes is the choice of the biosorbent material. The main criteria for the selection of the adsorbent/biosorbent are cost, removal capacity and selectivity. Thus, equilibrium studies are also an important aspect that demands proper attention in adsorption studies. Equilibrium data provide information about the biosorbent's performance, its maximum capacity of adsorption and selectivity, as well as some insights about the removal mechanism. In this work, experimental data for Ni^{2+} and Cr^{3+} adsorption equilibrium from single component solutions were obtained, and are shown in Figure 5.

From Figure 5, one can see that the *Sargassum filipendula* biomass adsorbs preferentially Cr^{3+} over Ni^{2+}. Its saturation value was two times higher than for Ni^{2+}. At lower concentrations, the equilibrium concentration of Cr^{3+} has higher than for Ni^{2+}. This pattern also repeats in others types of adsorbents. Results obtained by Barros *et al*. (2007), Farajzadeh and Monji (2004), and Rafatullah *et al*. (2009) also indicated that Cr^{3+} is adsorbed preferentially over Ni^{2+} in sanitary sewage, wheat bran, and meranti sawdust, respectively.

In addition to kinetic studies, mathematical modeling can also provide quantitative information about the equilibrium data obtained. For this purpose, the equilibrium data for Ni^{2+} and Cr^{3+} biosorption were used to fit the model parameters in the Langmuir and Sips isotherms. The Langmuir isotherm is frequently used to describe the equilibrium in mono-component systems, and is expressed by the following equation:

$$q_{eq} = \frac{q_{\max} b C_{eq}}{1 + b C_{eq}} \tag{18}$$

where: C_{eq} (meq.L^{-1}) is the ion concentration in the fluid phase at equilibrium, and b (L.meq^{-1}) and q_{max} (meq.g^{-1}) are adjustable parameters. The parameter b in Eq. (18) corresponds to the initial slope of the curve and indicates the biosorbent affinity for the adsorbed substance: a higher initial slope corresponds to a higher affinity constant. The parameter q_{max} is the Langmuir monolayer saturation capacity (maximum amount of adsorbate per unit weight of adsorbent to form a complete monolayer) (Ruthven, 1984).

The Sips or Langmuir-Freundlich isotherm is represented by the following equation:

$$q_{eq} = \frac{q_{\max} b C_{eq}^{k}}{1 + b C_{eq}^{k}} \tag{19}$$

where q_{max} and b have the same meaning as those in the Langmuir isotherm and the parameter k is a measure of the adsorbent heterogeneity. When $0 < k < 1$, the heterogeneity is considered to correspond to variations in the solid surface. When the adsorbed molecule has strong affinity for the adsorbent molecules (a positive cooperative effect), k will be greater than 1 (Tóth, 2001).

In this work, the isotherm parameters were determined using the Nelder and Mead (1965) method to minimize the objective function:

$$F_{OBJ} = \sum_{j=1}^{N} \left(\frac{C_{eq,j}^{EXP} - C_{eq,j}^{MOD}}{C_{eq,j}^{EXP}} \right)^2 \tag{20}$$

In Table 3 the isotherm parameters, r^2 and AAD are presented. The curves obtained using the isotherms are shown in Figure 5.

Table 3: Langmuir and Sips parameters for Cr^{3+} and Ni^{2+} mono-component adsorption by *Sargassum filipendula* algal biomass.

Model	Parameters	AAD	r^2
Langmuir			
Cr^{3+}	$q_m = 3.00$; $b = 3.28$	5.66	0.96
Ni^{2+}	$q_m = 1.48$; $b = 0.32$	3.70	0.97
Sips			
Cr^{3+}	$q_m = 3.12$; $b = 2.58$; $k = 0.90$	5.35	0.97
Ni^{2+}	$q_m = 1.23$; $b = 0.38$; $k = 1.34$	1.68	0.99

[q_m] = meq.g^{-1}; [b] = L.meq^{-1} (Langmuir); [b] = (L.meq^{-1})$^{-k}$ (Sips); [k] = dimensionless; [AAD] = %

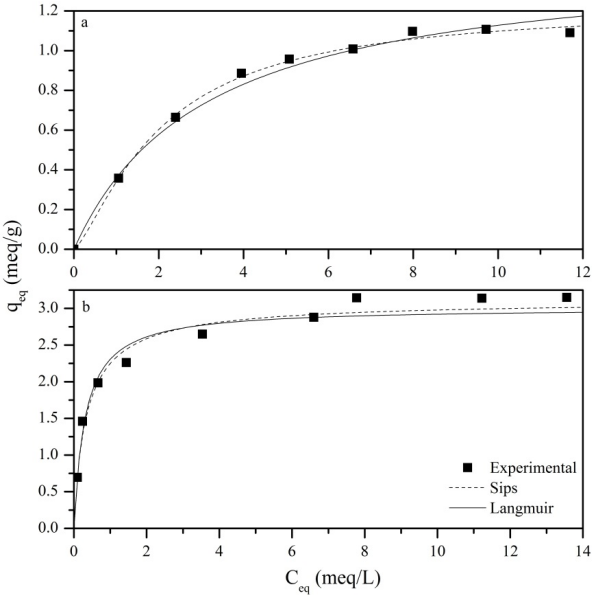

Figure 5: Individual equilibrium isotherm data for: (a) Ni^{2+} (b) Cr^{3+}.

From Table 3, one can see that, for the same metal, the Langmuir and Sips parameters do not differ significantly, which indicates that the biosorbent presents low heterogeneity. Also, the Sips isotherm fitted the experimental data better than the Langmuir model. This fact can be confirmed by the AAD and correlation coefficient values.

Indeed, the values of the Langmuir (and Sips) isotherm parameters confirmed that Cr^{3+} was adsorbed preferentially over Ni^{2+}. Both q_{max} and b presented higher values for Cr^{3+}. Also, the value of k in the Sips isotherm indicates that the biosorbent has high affinity for Cr^{3+} ($k > 1$).

In Table 4 are presented values for maximum uptake capacity for Cr^{3+} and Ni^{2+} removal in different adsorbents. Comparing these numbers with the ones obtained in this work, one can see that this biomass presents a good performance. Moreover, this seaweed species is abundant on the Brazilian coast and can be obtained at low coast. Therefore, *Sargassum filipendula* algal biomass has a high potential to be used in industrial adsorption processes for Cr^{3+}/Ni^{2+} removal.

Binary System

Adsorption equilibrium studies are also required for multi-component solutions. In this work, equilibrium data for Ni^{2+}/Cr^{3+} mixture adsorption were also obtained in order to complete this adsorption study. A comparison between Cr^{3+} and Ni^{2+} uptake in each experiment performed are presented in Figure 6.

The results obtained show that, for all binary adsorption experiments, the biosorbent selectivity remains $Cr^{3+} > Ni^{2+}$. Besides, the amount of Cr^{3+} adsorbed at equilibrium was at least three times higher than for Ni^{2+} in all experiments. This affinity order was also verified for different types of adsorbents. The results obtained by Parab *et al*. (2006), Sekhar *et al*. (1998), and Oliveira *et al*. (2005), who investigated the adsorption of solutions containing Cr^{3+} and other metallic ions, showed that this ion is preferentially adsorbed over the other ones in solution.

Table 4: Comparison of Cr^{3+} and Ni^{2+} maximum adsorption capacities on various adsorbents.

Biosorbent	q_m (meq/g)	pH	T (ºC)	Reference
Cr^{3+}				
Sargassum filipendula	3.12	3.0	30	This work
Vineyard pruning waste	0.718	4.2	30	Karaoğlu *et al*. (2010)
Rhodococcus opacus	2.808	5.0	25	Bueno *et al.* (2008).
Potamogeton lucens	1.290	5.5	25	Schneider and Rubio (1999).
Spirogyra spp.	1.743	5.0	25	Bishnoi *et al*. (2007).
Carrot residues	2.601	4.5	25	Nasernejad *et al*. (2005).
Ni^{2+}				
Sargassum filipendula	1.23	3.0	30	This work
Ulva reticulata	1.580	4.5	30	Vijayaraghavan *et al*. (2005).
Vegetative Bacillus thuringiensis	1.208	6.0	35	Öztürk (2007).
Spore-crystal mixture *Bacillus thuringiensis*	1.563	6.0	35	Öztürk (2007).
Sugarcane bagasse	0.068	5.0	25	Alomá *et al*. (2012)
Rhodotorula glutinis	1.514 2.130	7.5	25 70	(Suazo-Madrid *et al*., 2011)

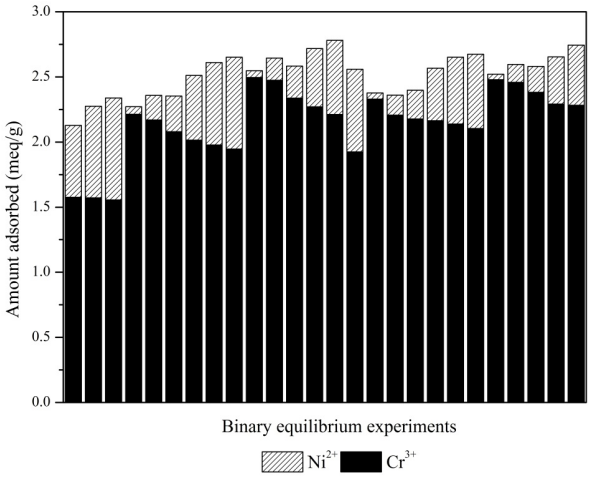

Figure 6: Equilibrium amount of Ni^{2+} and Cr^{3+} adsorbed from binary solutions.

Adsorption isotherms are also used to model binary equilibrium data and, over the last decades, several models were proposed. In this work, we modeled the experimental data using three isotherms: competitive Langmuir, competitive Langmuir-Freundlich and Jain and Snoeyink. The competitive form of the Langmuir isotherm is widely used to model multi-component equilibrium data. It is an extension obtained from the single component model. For binary systems, it can be described by the following equations (Ruthven, 1984):

$$q_{eq,1} = \frac{q_{\max,1} b_1 C_{eq,1}}{1 + b_1 C_{eq,1} + b_2 C_{eq,2}} \tag{21}$$

$$q_{eq,2} = \frac{q_{\max,2} b_2 C_{eq,2}}{1 + b_1 C_{eq,1} + b_2 C_{eq,2}} \tag{22}$$

where $q_{\max,1}$, and b_1 are the parameters calculated for the Cr^{3+} mono-component Langmuir isotherm and $q_{\max,2}$ and b_2 are the parameters calculated for the Ni^{2+} mono-component Langmuir isotherm. The Langmuir–Freundlich isotherm can be obtained by adding two new parameters (k_1, k_2) as concentration exponents in the Langmuir isotherm model (Ruthven, 1984):

$$q_{eq,1} = \frac{q_{\max,1} b_1 C_{eq,1}^{k_1}}{1 + b_1 C_{eq,1}^{k_1} + b_2 C_{eq,2}^{k_2}} \tag{23}$$

$$q_{eq,2} = \frac{q_{\max,2} b_2 C_{eq,2}^{k_2}}{1 + b_1 C_{eq,1}^{k_1} + b_2 C_{eq,2}^{k_2}} \tag{24}$$

The parameters of Eqs. (23) and(24) are derived from the mono-component Langmuir-Freundlich isotherm. Jain and Snoeyink (1973) proposed an adsorption model for binary mixtures based on the hypothesis that part of adsorption occurs without competition. If $q_{\max 1} > q_{\max 2}$, the mathematical expression can be written as:

$$q_{eq,1} = \frac{\left(q_{\max 1} - q_{\max 2}\right) b_1 C_{eq,1}}{1 + b_1 C_{eq,1}} + \frac{q_{\max 2} b_1 C_{eq,1}}{1 + b_1 C_{eq,1} + b_2 C_{eq,2}} \tag{25}$$

$$q_{eq,2} = \frac{q_{\max,2} b_2 C_{eq,2}}{1 + b_1 C_{eq,1} + b_2 C_{eq,2}} \tag{26}$$

All the parameters present in the Jain and Snoeyink isotherm are also derived from the mono-component Langmuir isotherm. Although this is a practice commonly used, the results obtained for mono-component systems generally do not predict the behavior of a binary system. This behavior is observed because the parameters do not take into account the interactions between the ions present (Repo *et al*., 2011). Aksu *et al*. (2002) proposed that an interaction parameter should be added to Eqs. (21)-(26) to characterize these effects. Thus, a modified form of the competitive Langmuir model can be written as:

$$q_{eq,1} = \frac{q_{\max,1} b_1 \left(C_{eq,1} / \eta_1\right)}{1 + b_1 \left(C_{eq,1} / \eta_1\right) + b_2 \left(C_{eq,2} / \eta_2\right)} \tag{27}$$

$$q_{eq,2} = \frac{q_{\max,2} b_2 \left(C_{eq,2} / \eta_2 \right)}{1 + b_1 \left(C_{eq,1} / \eta_1 \right) + b_2 \left(C_{eq,2} / \eta_2 \right)} \quad (28)$$

The modified Langmuir-Freundlich isotherm can be written as:

$$q_{eq,1} = \frac{q_{\max,1} b_1 \left(C_{eq,1}^{k_1} / \eta_1 \right)}{1 + b_1 \left(C_{eq,1}^{k_1} / \eta_1 \right) + b_2 \left(C_{eq,2}^{k_2} / \eta_2 \right)} \quad (29)$$

$$q_{eq,2} = \frac{q_{\max,2} b_2 \left(C_{eq,2}^{k_2} / \eta_2 \right)}{1 + b_1 \left(C_{eq,1}^{k_1} / \eta_1 \right) + b_2 \left(C_{eq,2}^{k_2} / \eta_2 \right)} \quad (30)$$

Finally, the modified form of the Jain and Snoeyink isotherm can be written as:

$$q_{eq,1} = \frac{\left(q_{\max 1} - q_{\max 2} \right) b_1 \left(C_{eq,1} / \eta_1 \right)}{1 + b_1 \left(C_{eq,1} / \eta_1 \right)} + \frac{q_{\max 2} b_1 \left(C_{eq,1} / \eta_1 \right)}{1 + b_1 \left(C_{eq,1} / \eta_1 \right) + b_2 \left(C_{eq,2} / \eta_2 \right)} \quad (31)$$

$$q_{eq,2} = \frac{q_{\max,2} b_2 \left(C_{eq,2} / \eta_2 \right)}{1 + b_1 \left(C_{eq,1} / \eta_1 \right) + b_2 \left(C_{eq,2} / \eta_2 \right)} \quad (32)$$

In Eqs. (27)-(32) only the dimensionless interaction parameters, η_1 and η_2, should be estimated using the binary equilibrium data by solving simultaneously both equations. All the others are derived similarly to the conventional models. In this work, the interaction parameters were calculated using the Nelder and Mead (1965) method to minimize the objective function:

$$F_{OBJ} = \sum_{i=1}^{2} \sum_{j=1}^{N} \left(\frac{C_{eq,i,j}^{EXP} - C_{eq,i,j}^{MOD}}{C_{eq,i,j}^{EXP}} \right)^2 \quad (33)$$

where $i = 1$ correspond to Cr^{3+} ions and $i = 2$, to Ni^{2+}. The parameters $q_{\max,1}$, $q_{\max,2}$, b_1, and b_2 were taken from the mono-component results (Table 3). The interaction parameters obtained for each binary isotherm, AAD and r^2 calculated for each ion are shown in Table 5.

The values of η_i obtained deviate from unity in all cases. This indicates that the parameters obtained by using the mono-component isotherms would not lead to good predictions if used in multi-component models. The model that best fitted the experimental data was the modified Langmuir-Freundlich isotherm, for which the calculated AAD were 8.30% and 26.2% for Cr^{3+} and Ni^{2+}, respectively.

An affinity parameter, B_i, can also be calculated for binary isotherms and is given by the product $\eta_i \, x \, b_i$. The values of B_i are also shown in Table 5, where one can see that, for all binary models: $B_{Cr^{3+}} > B_{Ni^{2+}}$. This result confirms that Cr^{3+} has an inhibitory effect over Ni^{2+}.

It has been reported that brown seaweeds present several functional groups, such as: carboxyl/hydroxyl groups in alginic acid, amine/amide groups in the peptidoglycans and proteins, and sulfonate and thiol groups in the sulfate polysaccharides and amino acids (Raize *et al*., 2004). All these groups are known to bind heavy metals.

Infrared spectra obtained by Fourier transform infrared spectrometry (FT-IR) can be used to determine which functional groups play a role in adsorption processes. In the literature it has been reported that Ni^{2+} ions can be bonded by: amine, amide, carboxyl, hydroxyl, and sulfonate groups (Kleinübing *et al*., 2010; Çelekli and Bozkurt, 2011; Ramana *et al*., 2012).

Table 5: Adsorption isotherm model parameters and statistical parameters calculated for Cr^{3+}/Ni^{2+} mixture adsorption. The values between parentheses are statistical parameters calculated using Eqs. (21)-(26).

Models	Parameters	AAD	r^2
1. Modified Langmuir	$\eta_1 = 1.129$; $B_1 = 3.70$ $\eta_2 = 1.634$; $B_2 = 0.52$	1: 10.2 2: 35.9	1: 0.93 2: 0.87
2. Modified Jain and Snoeyink	$\eta_1 = 2.161$; $B_1 = 7.09$ $\eta_2 = 2.851$; $B_2 = 0.91$	1: 8.30 2: 35.9	1: 0.91 2: 0.89
3. Modified Langmuir-Freundlich	$\eta_1 = 0.514$; $B_1 = 1.33$ $\eta_2 = 1.694$; $B_2 = 0.64$	1: 12.8 2: 26.2	1: 0.91 2: 0.92

Index 1 refers to $Cr^{3+}$and index 2 to Ni^{2+}. [η_2] = dimensionless; [B_i] = L.meq^{-1}; [AAD] = %

In other studies it has been found that Cr^{3+} ions can be bound by carboxyl, hydroxyl, aldehyde, amine, phosphate, thiol, and ether groups (Karaoğlu *et al*., 2010; Dos Santos Lima *et al*., 2011; Fathima *et al*., 2012). As mentioned above, several of these groups are present in *Sargassum filipendula*'s surface and the inhibition of Ni^{2+} removal by Cr^{3+} ions is probably caused by the competition of both ions for the same functional group.

In Figures 8a-c are shown the relation between the experimental q_{eq} and the ones calculated by the isotherm models. Also, a comparison between the original and modified models is presented. If the results for conventional and modified isotherms were similar, the open and filled symbols should overlap. From these graphs, it is evident that there is a difference between the two modeling approaches. The results obtained from the original and modified competitive Langmuir isotherms show that they were practically equivalent. For the Jain and Snoeyink isotherm, the results obtained for the modified model were slightly better for Cr^{3+}, and almost equivalent for Ni^{2+}. However, for the Langmuir-Freundlich isotherm the results obtained for the modified one were significantly better when compared to the original model. This fact corroborates the importance of estimating the interaction parameters in multi-component adsorption processes.

Modeling adsorption equilibria of binary solutions is still a challenge. Several studies that suffer from bad predictions can be found on the literature. For example, Fagundes-Klen *et al*. (2007) used several adsorption isotherms to model the removal of Cd^{2+}/Zn^{2+} mixtures by *Sargassum filipendula* and obtained poor predictions. Luna *et al*. (2010) modeled Cd^{2+}/Zn^{2+} biosorption onto *Sargassum filipendula* and obtained errors between 16.5% and 37.4%. Also, Repo *et al*. (2011) obtained errors between 15% and 140% when modeling Co^{2+}/Ni^{2+} adsorption onto EDTA- and DTPA-modified silica gel.

To improve the quality of data fitting, Jha and Madras (2005) proposed that another modeling tool could be used: Artificial Neural Networks (ANNs). ANNs are mathematical algorithms that have the capacity to relate independent to dependent variables of a process by learning from given examples, without requesting any knowledge about the mathematical formulation of the process.

An ANN is based on the structure of the biological neuronal system and consists basically of a set of artificial neurons that are interconnected and organized into layers. The information process in an ANN begins by relating the input (x_i) of each neuron to a synaptic weight (w_{ij}) that assesses the influence of this entry on the output of this neuron (activation coefficients). The sum of all the activation coefficients causes the neuron activation. The answer of the input stimulus is obtained by applying an activation function to the neuron activation, generally the sigmoid or the hyperbolic tangent function. This procedure extends to the output layer of the network, where the ANN answers are the dependent variables of the problem (Braga *et al*., 2000).

The determination of the network structure is not a simple task: there is no rule or theorem to find the optimal topology of a network for a given data set. Modeling with ANNs consists of varying the number of neurons of the input and hidden layers to find the suitable synaptic weights that minimize the deviation among observed and calculated data. This process consists of a step called network training and it is in this step that the network learning is evaluated. ANNs have been widely used in problems concerning food processing, process control, phase equilibrium, and biotechnological processes (Schmitz *et al*., 2006; Rivera *et al*., 2007; da Cruz *et al*., 2009). In the adsorption field, ANNs were successfully used to model several multi-component systems (Carsky and Do, 1999; Jha and Madras, 2005; Fagundes-Klen *et al*., 2007; Canevesi *et al*., 2012).

To illustrate that ANNs could be used to describe the equilibrium of binary adsorption processes, we used feedforward ANNs with two hidden layers to model the data from Cr^{3+}/Ni^{2+} mixture biosorption. The input variables were the equilibrium concentrations of Cr^{3+} and Ni^{2+} in the fluid phase, while the uptake amount of Cr^{3+} and Ni^{2+} were used as output. A schematic diagram of the ANN structures tested is shown in Figure 7.

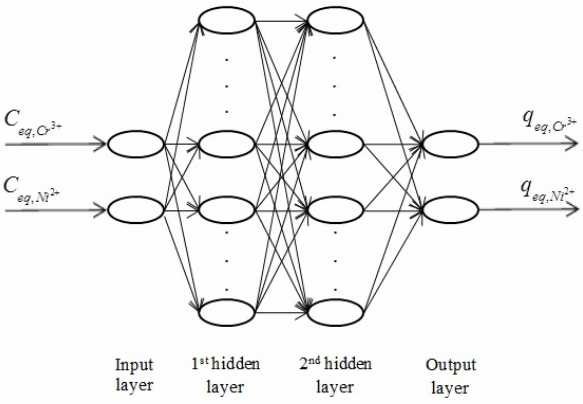

Figure 7: Schematic diagram of the ANNs tested in this work.

To obtain the ANN structure that better fit the

experimental data, different numbers of neuron combinations were tested in the hidden layers (from 2 to 10). To estimate the value of the synaptic weights, the Simulated Annealing method (Albrecht and Wong, 2001) was used to minimize the objective function given by Eq. (33). The hyperbolic secant (hidden layers) and linear function (output layer) were used as activation functions. All the simulations were conducted with our own Fortran code.

Once the synaptic weights are determined, the next step is to validate the model. Usually, this is performed by presenting new data to the network and comparing the new outputs with the corresponding experimental ones. Since we have only 26 experimental data and the objective is to suggest a new tool that to be used to model binary equilibrium data, we choose to use all 26 data collected to train the ANN and perform a preliminary study. Further experiments will be performed in the future in order to do an extensive study related to neural network modeling in adsorption processes.

Among all network architectures considered, the best results were obtained using ANNs with two hidden layers and two neurons in the second hidden layer. In Table 6 are shown the objective function, the AAD and the r^2 obtained for these structures. From these values, one can see that the ANN modeling is superior when compared to the isotherm performance. The simplest ANN architecture (2-2-2-2) was able to describe the equilibrium data with success. The best result was achieved by the ANN with 2 neurons in the first hidden layer and 8 neurons in the second hidden layer. The AAD obtained were 2.15 % and 6.72 % for Cr^{3+} and Ni^{2+}, respectively. In Figure 8d the relation between the experimental q_{eq} and the values calculated by the ANN 2-8-2-2 is shown and the better performance obtained from the ANN modeling can be confirmed.

Table 6: Values of the objective function and AAD obtained using different architectures in the artificial neural network.

Architecture	F_{Obj}	AAD	r^2
2-2 2 2	1.415	1: 4.64 2: 14.90	1: 0.95 2: 0.86
2-4 2 2	0.860	1: 2.89 2: 8.72	1: 0.97 2: 0.93
2-6 2 2	0.637	1: 2.15 2: 8.95	1: 0.97 2: 0.91
2-8 2 2	0.486	1: 2.15 2: 6.72	1: 0.97 2: 0.94

Index 1 refers to $Cr^{3+}$and index 2 to Ni^{2+}; [AAD] = %.

The accuracy obtained using ANN modeling is mainly due to the versatility of the technique. The ANN algorithm is based on the functioning of the human brain. Their principal feature is that they can relate input and output variables without requiring a detailed mathematical knowledge of the process. Thus, an ANN can be used to model almost any known process. On the other hand, isotherm models are based on several hypotheses that often are not related to the reality of any experiment (e.g.: homogeneous adsorbent hypotheses of the Langmuir isotherm). Its formulation is complicated because biosorption processes are usually a combination of adsorption, ion exchange, complexation, quelation, etc. and its application is limited to specific cases. Regarding this work, it seems that ANN may be a promising tool due to the uncertainties in the mechanism of Cr^{3+}/Ni^{2+} removal, that would be needed for multi-component isotherm formulation.

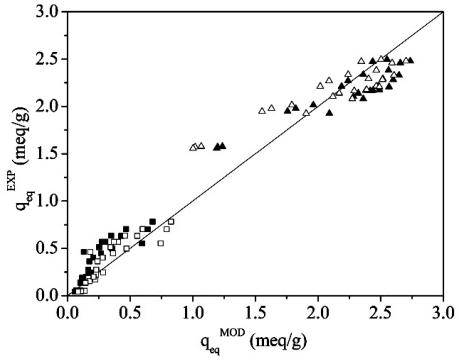

(a)

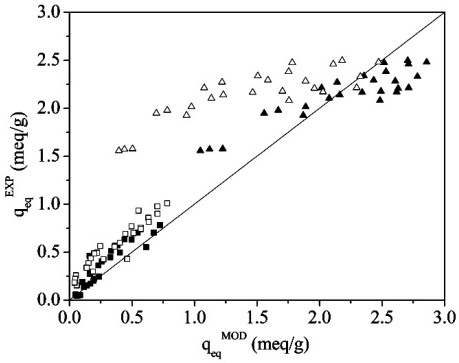

(b)

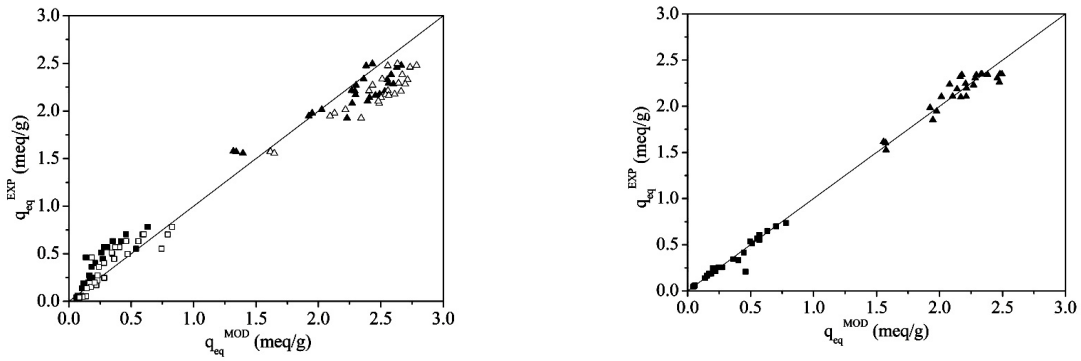

(c) (d)

Figure 8: Relation between the experimental equilibrium adsorption capacities and those calculated by the modified (a) Langmuir, (b) Langmuir-Freundlich, (c) Jain and Snoeyink, isotherm models, and (d) ANN 2-8-8-2. Triangles represent Cr^{3+}. Squares represent Ni^{2+}. Open and filled symbols are results from the original modified isotherm models, respectively.

CONCLUSION

In this work mono- and multi-component biosorption of Cr^{3+} and Ni^{2+} ions by *Sargassum filipendula* pre-treated with $CaCl_2$ was investigated. Kinetic and equilibrium studies were performed for both systems. A simple comparison with other studies showed that the algae biomass has great potential for use in a process unit. Our results showed that Cr^{3+} adsorption kinetics were slower than for Ni^{2+} in both mono-component and binary experiments. A mechanistic analysis revealed that this difference could be attributed to the number of adsorption stages of each metallic ion: Cr^{3+} uptake presented three adsorption stages, whereas for Ni^{2+} there are only two. A strong competitive behavior was observed in binary studies: when both ions are present in solution, Ni^{2+} ions were gradually removed from the biomass. Besides, the higher the initial concentration of Cr^{3+}, the higher the Ni^{2+} desorption. Equilibrium experiments confirmed that Cr^{3+} is preferentially adsorbed by the biosorbent in both mono- and multi-component experiments. Finally, results obtained by using adsorption isotherms showed that these models fail to describe the binary equilibrium. On the other hand, preliminary simulations with Artificial Neural Networks showed that they could be a viable alternative to model complex processes, such as the adsorption of heavy metals using natural materials as adsorbents.

REFERENCES

Aksu, Z., AçIkel, Ü., Kabasakal, E., Tezer, S., Equilibrium modelling of individual and simultaneous biosorption of chromium(VI) and nickel(II) onto dried activated sludge. Water Research, 36 (12), p. 3063-3073 (2002).

Al-Homaidan, A. A., Accumulation of nickel by marine macroalgae from the Saudi coast of the Arabian Gulf. Journal of Food, Agriculture and Environment, 6(1), p. 148-151 (2008).

Albrecht, A., Wong, C. K., Combining the perceptron algorithm with logarithmic simulated annealing. Neural Process. Lett., 14(1), p. 75-83 (2001).

Alkan, M., Dogan, M., Turhan, Y., Demirbas, Ö., Turan, P., Adsorption kinetics and mechanism of maxilon blue 5G dye on sepiolite from aqueous solutions. Chemical Engineering Journal, 139(2), p. 213-223 (2008).

Alomá, I., Martín-Lara, M. A., Rodríguez, I. L., Blázquez, G., Calero, M., Removal of nickel (II) ions from aqueous solutions by biosorption on sugarcane bagasse. Journal of the Taiwan Institute of Chemical Engineers, 43(2), p. 275-281 (2012).

Anoop Krishnan, K., Sreejalekshmi, K. G., Baiju, R. S., Nickel(II) adsorption onto biomass based activated carbon obtained from sugarcane bagasse pith. Bioresource Technology, 102(22), p. 10239-10247 (2011).

Aravindhan, R., Aafreen Fathima, A. F., Selvamurugan, M., Raghava Rao, J., Balachandran, U., Adsorption, desorption, and kinetic study on Cr(III) removal from aqueous solution using *Bacillus subtilis* biomass. Clean Technologies and Environmental Policy, p. 1-9 (2012). (In Press).

Barros, A. J. M., Prasad, S., Leite, V. D., Souza, A. G., Biosorption of heavy metals in upflow sludge columns. Bioresource Technology, 98(7), p. 1418-1425 (2007).

Bishnoi, N. R., Kumar, R., Kumar, S., Rani, S., Biosorption of Cr(III) from aqueous solution using algal biomass spirogyra spp. Journal of Hazardous Materials, 145(1-2), p. 142-147 (2007).

Braga, A. P., Carvalho, A. P. L., Ludermir, T. B., Redes Neurais Artificiais: Teoria e Aplicações. Rio de Janeiro: LTC – Livros Técnicos e Científicos (2000). (In Portuguese).

Bueno, B. Y. M., Torem, M. L., Molina, F., de Mesquita, L. M. S., Biosorption of lead(II), chromium(III) and copper(II) by R. opacus: Equilibrium and kinetic studies. Minerals Engineering, 21(1), p. 65-75 (2008).

Calero, M., Hernáinz, F., Blázquez, G., Martín-Lara, M. A., Tenorio, G., Biosorption kinetics of Cd (II), Cr (III) and Pb (II) in aqueous solutions by olive stone. Brazilian Journal of Chemical Engineering, 26, p. 265-273 (2009).

Canevesi, R. L. S., Junior, E. A. Z., Barella, R. A., Martins, T. D., Moreira, M. F. P., da Silva, E. A., Prediction of ternary ion-exchange equilibrium using artificial neural networks and law of mass action. Acta Scientiarum: Technology, 34(1), p. 53-60 (2012).

Carsky, M., Do, D. D., Neural network modeling of adsorption of binary vapour mixtures. Adsorption, 5(3), p. 183-192 (1999).

Çelekli, A., Bozkurt, H., Bio-sorption of cadmium and nickel ions using *Spirulina platensis*: Kinetic and equilibrium studies. Desalination, 275(1-3), p. 141-147 (2011).

Chen, J. H., Li, G. P., Liu, Q. L., Ni, J. C., Wu, W. B., Lin, J. M., Cr(III) ionic imprinted polyvinyl alcohol/sodium alginate (PVA/SA) porous composite membranes for selective adsorption of Cr(III) ions. Chemical Engineering Journal (Lausanne), 165(2), p. 465-473 (2010).

Choi, J.-W., Choi, N.-C., Lee, S.-J., Kim, D.-J., Novel three-stage kinetic model for aqueous benzene adsorption on activated carbon. Journal of Colloid and Interface Science, 314(2), p. 367-372 (2007).

da Cruz, A. G., Walter, E. H. M., Cadena, R. S., Faria, J. A. F., Bolini, H. M. A., Frattini Fileti, A. M., Monitoring the authenticity of low-fat yogurts by an artificial neural network. Journal of Dairy Science, 92(10), p. 4797-4804, October 1, 2009 (2009).

Dos Santos Lima, L. K., Kleinübing, S. J., Da Silva, E. A., Da Silva, M. G. C., Removal of chromium from wastewater using macrophyte lemna minor as biosorbent. Chemical Engineering Transactions, 25, p. 303-308 (2011).

Fagundes-Klen, M. R., Ferri, P., Martins, T. D., Tavares, C. R. G., Silva, E. A., Equilibrium study of the binary mixture of cadmium-zinc ions biosorption by the *Sargassum filipendula* species using adsorption isotherms models and neural network. Biochemical Engineering Journal, 34(2), p. 136-146 (2007).

Fahim, N. F., Barsoum, B. N., Eid, A. E., Khalil, M. S., Removal of chromium(III) from tannery wastewater using activated carbon from sugar industrial waste. Journal of Hazardous Materials, 136(2), p. 303-309 (2006).

Farajzadeh, M. A., Monji, A. B., Adsorption characteristics of wheat bran towards heavy metal cations. Separation and Purification Technology, 38(3), p. 197-207 (2004).

Farooq, U., Kozinski, J. A., Khan, M. A., Athar, M., Biosorption of heavy metal ions using wheat based biosorbents – A review of the recent literature. Bioresource Technology, 101(14), p. 5043-5053 (2010).

Fathima, A., Rao, J. R., Unni Nair, B., Trivalent chromium removal from tannery effluent using kaolin-supported bacterial biofilm of Bacillus sp isolated from chromium polluted soil. Journal of Chemical Technology and Biotechnology, 87(2), p. 271-279 (2012).

Fernandes, S., Gando-Ferreira, L. M., Kinetic modeling analysis for the removal of Cr(III) by Diphonix resin. Chemical Engineering Journal (Lausanne), 172(2-3), p. 623-633 (2011).

Hajar, M., Biosorption of cadmium from aqueous solution using dead biomass of brown alga Sargassum Sp. Chemical Engineering Transactions, 17, p. 1173-1178 (2009).

Ho, Y. S., McKay, G., Kinetic models for the sorption of dye from aqueous solution by wood. Process Safety and Environmental Protection, 76(2), p. 183-191 (1998).

Ijagbemi, C. O., Baek, M.-H., Kim, D.-S., Adsorptive performance of un-calcined sodium exchanged and acid modified montmorillonite for Ni2+ removal: Equilibrium, kinetics, thermodynamics and regeneration studies. Journal of Hazardous Materials, 174(1-3), p. 746-755 (2010).

Jain, J. S., Snoeyink, V. L., Adsorption from bisolute systems on active carbon. Journal of the Water Pollution Control Federation, 45(12), p. 2463-2479 (1973).

Jha, S. K., Madras, G., Neural network modeling of adsorption equilibria of mixtures in supercritical fluids. Industrial & Engineering Chemistry Research, 44(17), p. 7038-7041 (2005).

Karaoğlu, M. H., Zor, Ş., Uğurlu, M., Biosorption of Cr(III) from solutions using vineyard pruning

waste. Chemical Engineering Journal (Lausanne), 159(1-3), p. 98-106 (2010).

Kleinübing, S. J., Vieira, R. S., Beppu, M. M., Guibal, E., Silva, M. G. C., Characterization and evaluation of copper and nickel biosorption on acidic algae *Sargassum filipendula*. Materials Research, 13, p. 541-550 (2010).

Lagergren, S., Kungliga Svenska Vetenskapsakademiens. Handlingar, 24, p. 1 (1898).

Luna, A. S., Costa, A. L. H., da Costa, A. C. A., Henriques, C. A., Competitive biosorption of cadmium(II) and zinc(II) ions from binary systems by *Sargassum filipendula*. Bioresource Technology, 101(14), p. 5104-5111 (2010).

Malash, G. F., El-Khaiary, M. I., Piecewise linear regression: A statistical method for the analysis of experimental adsorption data by the intraparticle-diffusion models. Chemical Engineering Journal (Lausanne), 163(3), p. 256-263 (2010).

Matheickal, J. T., Yu, Q., Biosorption of lead(II) and copper(II) from aqueous solutions by pre-treated biomass of Australian marine algae. Bioresource Technology, 69(3), p. 223-229 (1999).

Matheickal, J. T., Yu, Q., Woodburn, G. M. Biosorption of cadmium(II) from aqueous solutions by pre-treated biomass of marine alga *Durvillaea potatorum*. Water Research, 33(2), p. 335-342 (1999).

Nasernejad, B., Zadeh, T. E., Pour, B. B., Bygi, M. E., Zamani, A., Comparison for biosorption modeling of heavy metals (Cr (III), Cu (II), Zn (II)) adsorption from wastewater by carrot residues. Process Biochemistry, 40(3-4), p. 1319-1322 (2005).

Nehrenheim, E., Gustafsson, J. P., Kinetic sorption modelling of Cu, Ni, Zn, Pb and Cr ions to pine bark and blast furnace slag by using batch experiments. Bioresource Technology, 99(6), p. 1571-1577 (2008).

Nelder, J. A., Mead, R., A simplex method for function minimization. The Computer Journal, 7(4), p. 308-313, January 1, 1965 (1965).

Nuhoglu, Y., Malkoc, E., Thermodynamic and kinetic studies for environmentaly friendly Ni(II) biosorption using waste pomace of olive oil factory. Bioresource Technology, 100(8), p. 2375-2380 (2009).

Oliveira, E. A., Montanher, S. F., Andrade, A. D., Nóbrega, J. A., Rollemberg, M. C., Equilibrium studies for the sorption of chromium and nickel from aqueous solutions using raw rice bran. Process Biochemistry, 40(11), p. 3485-3490 (2005).

Öztürk, A., Removal of nickel from aqueous solution by the bacterium *Bacillus thuringiensis*. Journal of Hazardous Materials, 147(1-2), p. 518-523 (2007).

Parab, H., Joshi, S., Shenoy, N., Lali, A., Sarma, U. S., Sudersanan, M., Determination of kinetic and equilibrium parameters of the batch adsorption of Co(II), Cr(III) and Ni(II) onto coir pith. Process Biochemistry, 41(3), p. 609-615 (2006).

Rafatullah, M., Sulaiman, O., Hashim, R., Ahmad, A., Adsorption of copper(II), chromium(III), nickel(II) and lead(II) ions from aqueous solutions by meranti sawdust. Journal of Hazardous Materials, 170(2-3), p. 969-977 (2009).

Raize, O., Argaman, Y., Yannai, S., Mechanisms of biosorption of different heavy metals by brown marine macroalgae. Biotechnology and Bioengineering, 87(4), p. 451-458 (2004).

Ramana, D. K. V., Reddy, D. H. K., Kumar, B. N., Harinath, Y., Seshaiah, K., Removal of nickel from aqueous solutions by citric acid modified Ceiba pentandra hulls: Equilibrium and kinetic studies. The Canadian Journal of Chemical Engineering, 90(1), p. 111-119 (2012).

Repo, E., Petrus, R., Sillanpää, M., Warchoł, J. K., Equilibrium studies on the adsorption of Co(II) and Ni(II) by modified silica gels: One-component and binary systems. Chemical Engineering Journal (Lausanne), 172(1), p. 376-385 (2011).

Rivera, E. C., Costa, A. C., Andrade, R. R., Atala, D. I. P., Maugeri, F., Maciel Filho, R., Development of adaptive modeling techniques to describe the temperature-dependent kinetics of biotechnological processes. Biochemical Engineering Journal, 36(2), p. 157-166 (2007).

Rocha, S. C. S., de Assis Cavalcante, J., da Silva, M. G. C., Gonçalves Pinho, C., Influence of the drying conditions of Sargassum sp. alga on the bioadsorption of hexavalent chromium. Environmental Technology, 27(9), p. 979-990 (2006).

Ruthven, D. M., Principles of Adsorption and Desorption Processes. New York: John Wiley & Sons (1984).

Schmitz, J. E., Zemp, R. J., Mendes, M. J., Artificial neural networks for the solution of the phase stability problem. Fluid Phase Equilibria, 245(1), p. 83-87 (2006).

Schneider, I. A. H., Rubio, J., Sorption of heavy metal ions by the nonliving biomass of freshwater macrophytes. Environmental Science & Technology, 33 (13), p. 2213-2217 (1999).

Sekhar, K. C., Subramanian, S., Modak, J. M., Natarajan, K. A., Removal of metal ions using an industrial biomass with reference to environmental control. International Journal of Mineral Processing, 53(1-2), p. 107-120 (1998).

Silva, E. A., Cossich, E. S., Tavares, C. G., Cardozo

Filho, L., Guirardello, R., Biosorption of binary mixtures of Cr(III) and Cu(II) ions by Sargassum sp. Brazilian Journal of Chemical Engineering, 20, p. 213-227 (2003).

Sivaprakash, B., Rajamohan, N., Mohamed Sadhik, A., Batch and column sorption of heavy metal from aqueous solution using a marine alga *Sargassum tenerrimum*. International Journal of ChemTech Research, 2(1), p. 155-162 (2010).

Srivastava, V. C., Mall, I. D., Mishra, I. M., Competitive adsorption of cadmium(II) and nickel(II) metal ions from aqueous solution onto rice husk ash. Chemical Engineering and Processing: Process Intensification, 48(1), p. 370-379 (2009).

Suazo-Madrid, A., Morales-Barrera, L., Aranda-García, E., Cristiani-Urbina, E., Nickel(II) biosorption by *Rhodotorula glutinis*. Journal of Industrial Microbiology & Biotechnology, 38(1), p. 51-64 (2011).

Tóth, J., Adsorption, Theory, Modeling, and Analysis. 1st Ed. New York: Marcel Dekker Inc. (2001).

Tsui, M. T. K., Cheung, K. C., Tam, N. F. Y., Wong, M. H., A comparative study on metal sorption by brown seaweed. Chemosphere, 65(1), p. 51-57 (2006).

Vieira, M. G. A., Almeida Neto, A. F. d., Silva, M. G. C. d., Nóbrega, C. C., Melo Filho, A. A., Characterization and use of in natura and calcined rice husks for biosorption of heavy metals ions from aqueous effluents. Brazilian Journal of Chemical Engineering, 29, p. 619-634 (2012).

Vijayaraghavan, K., Jegan, J., Palanivelu, K., Velan, M., Biosorption of copper, cobalt and nickel by marine green alga Ulva reticulata in a packed column. Chemosphere, 60(3), p. 419-426 (2005).

Volesky, B., Holan, Z. R., Biosorption of heavy metals. Biotechnology Progress, 11(3), p. 235-250 (1995).

Weber, W. J., Morris, J. C., Kinetics of adsorption on carbon from solution. J. Sanit. Eng. Div. ASCE, 89 (SA2), p. 31-59 (1963).

Wilczak, A., Keinath, T. M., Kinetics of sorption and desorption of copper(II) and lead(II) on activated carbon. Water Environment Research, 65(3), p. 238-244 (1993).